

2.6.2 Diagnosis of early cancer and precancerous lesions with single-scattered light

The single scattering component of the returned light contains information about the structure of the uppermost epithelial cells. It has been shown that LSS enables quantitative characterization of some of the most important changes in tissues associated with precancerous and early cancerous transformations, namely, enlargement and crowding of epithelial cell nuclei.^{10,11,49} As discussed above, typical nondysplastic epithelial cell nuclei range in size from 4 to 10 μm . In contrast, dysplastic and malignant cell nuclei can be as large as 20 μm . Single scattering events from such particles, which are large compared to the wavelength of visible light (0.5 to 1 μm), can be described by the Mie theory. This theory predicts that the scattered light undergoes small but significant spectral variations. In particular, the spectrum of scattered light contains a component that oscillates as a function of wavelength (see Sec. 2.3.2). The frequency of these oscillations is proportional to the particle size. Typically, normal nuclei undergo one such oscillation cycle as the wavelength varies from blue to red, whereas dysplastic/malignant nuclei exhibit up to two such oscillatory cycles. Such spectral features were observed in the white light directly backscattered from the uppermost epithelial cell nuclei in human mucosae.¹⁰

When the epithelial nuclei are distributed in size, the resulting signal is a superposition of these single frequency oscillations, with amplitudes proportional to the number of particles of each size. Thus, the nuclear size distribution can be obtained from the amplitude of the inverse Fourier transform of the oscillatory component of light scattered from the nuclei.¹⁰ Once the nuclear size distribution is known, quantitative measures of nuclear enlargement (shift of the distribution toward larger sizes) and crowding (increase in area under the distribution) can be obtained. This information quantifies the key features used by pathologists in the histologic diagnosis of dysplasia and CIS, and can be important in assessing premalignant and noninvasive malignant changes in biological tissue *in situ*.

However, single scattering events cannot be directly observed in *in vivo* tissues. Only a small portion of the light incident on the tissue is directly backscattered. The rest enters the tissue and undergoes multiple scattering from a variety of tissue constituents where it becomes randomized in direction, producing a large background of diffusely scattered light. Light returned after a single scattering event must be distinguished from this diffuse background. This requires special techniques because the diffusive background itself exhibits prominent spectral features dominated by the characteristic absorption bands of hemoglobin and the scattering of collagen fibers, which are in abundance in the connective tissue lying below the epithelium.

Several methods to distinguish single scattering have been proposed. Field-based light scattering spectroscopy⁵⁰ and spectroscopic optical

coherence tomography⁵¹ were developed for performing cross-sectional tomographic and spectroscopic imaging. In these extensions of conventional optical coherence tomography (OCT),⁵² information on the spectral content of backscattered light is obtained by detection and processing of the interferometric OCT signal. These methods allow the spectrum of backscattered light to be measured either for several discrete wavelengths,⁵⁰ or simultaneously over the entire available optical bandwidth from 650 to 1000 nm⁵¹ in a single measurement.

Another method⁴⁹ is based on the fact that initially polarized light loses its polarization when traversing a turbid medium such as biological tissue. Consider a mucosal tissue illuminated by linearly polarized light. A small portion of the incident light will be backscattered by the epithelial cell nuclei. The rest of the signal diffuses into the underlying tissue and is depolarized by multiple scattering. In contrast, the polarization of the light scattered backward after a single scattering event is preserved. Thus, by subtracting the unpolarized component of the reflected light, the contribution due to the backscattering from epithelial cell nuclei can be readily distinguished. The residual spectrum can then be analyzed to extract the size distribution of the nuclei, their population density, and their refractive index.

This method was implemented as follows: collimated polarized light from a broadband source is delivered on a tissue sample. The returned light is split into two orthogonally polarized signals, I_{\parallel} with the polarization vector parallel to that of the incident light and I_{\perp} with the perpendicular polarization vector, by means of a broadband polarizing beamsplitter cube. The output from this cube is delivered through optical fibers into two channels of a multichannel spectroscope (Fig. 2.16). This enables the spectra of both components, I_{\parallel} and I_{\perp} , to be simultaneously measured in the range of 400 to 900 nm. The experiments have shown that taking away the unpolarized component of the reflected light by means of subtracting I_{\perp} from I_{\parallel} allowed the single scattering component to be accurately restored.

The applicability of the technique to biological tissues was tested in studies with normal and cancerous human colon tissue samples obtained immediately after surgical resection. Figure 2.17 shows the size and refractive index distributions of the epithelial cell nuclei obtained for normal and cancerous tissue samples. For the normal tissue sample, the average diameter was found to be $d = 4.8 \mu\text{m}$, the standard deviation of the sizes was $\sigma = 0.4 \mu\text{m}$, and the relative refractive index of the nuclei was $m = 1.035$. For the cancerous tissue sample, the corresponding values were $d = 9.75 \mu\text{m}$, $\sigma = 1.5 \mu\text{m}$, and $m = 1.045$.

As can be seen in Fig. 2.17, the populations of normal and cancerous cell nuclei are clearly distinguishable. Cancerous nuclei are noticeably enlarged and have a higher refractive index. The increase in the nuclear refractive index from normal to cancerous tissue is also characteristic. As mentioned earlier, cancerous and dysplastic nuclei are known to stain darker than benign nuclei

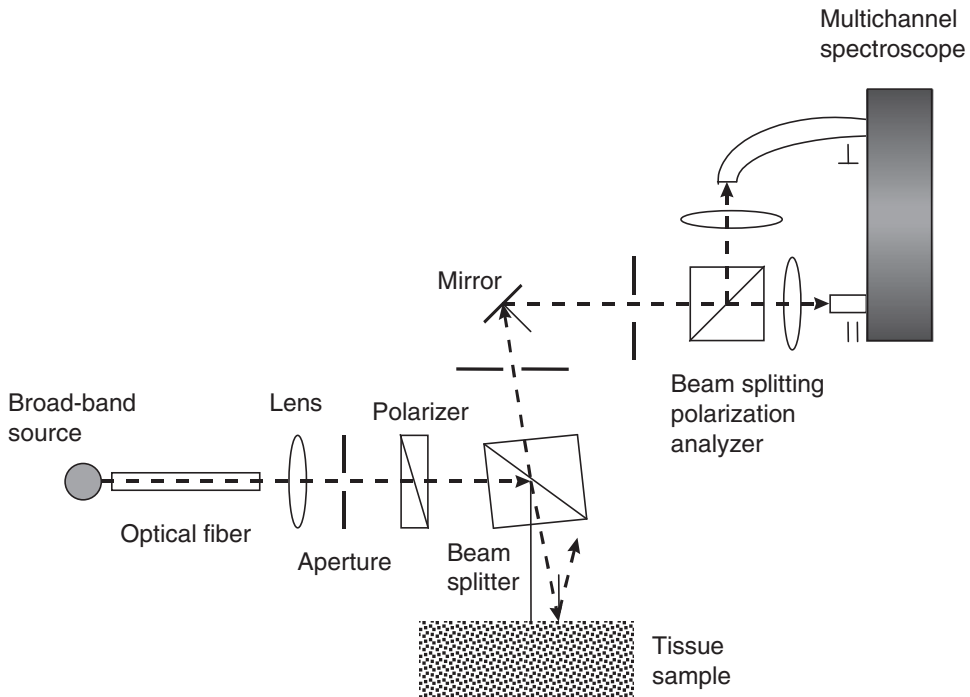


Figure 2.16 Schematic diagram of polarization LSS system.

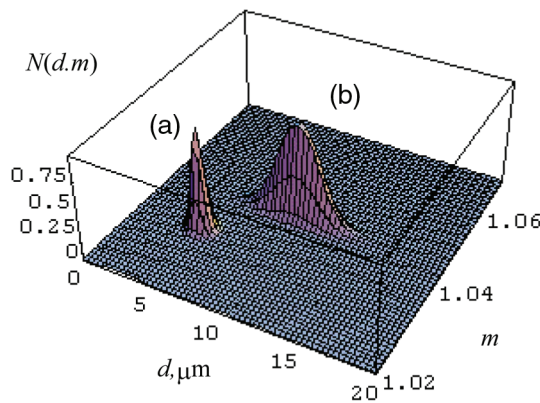


Figure 2.17 Size distributions and refractive index distributions, $N(d,m)$, of epithelial cell nuclei obtained with LSS for the (a) normal and (b) cancerous colon tissue samples.

(hyperchromaticity). This suggests a higher concentration of nuclear solids such as DNA, RNA, and proteins within the cancerous nuclei. Studies have shown that the refractive index of a cell organelle increases linearly with the concentration of its solid components. Therefore, a higher value of the refractive index obtained for the cancerous nuclei is indicative of nuclear hyperchromaticity.

The third method of diffusive background removal is based on the observation that this background is typically responsible for more than 95–98% of the total reflectance signal. Therefore, the diffusive background is responsible for the coarse features of the reflectance spectra. The diffusion approximation-based model discussed above may account for this component by fitting to its coarse features. After the model fit is subtracted, the single backscattering component becomes apparent and can be further analyzed to obtain the nuclear size distribution.¹⁰ This method is simpler to implement, because it does not require the use of polarized light, but is computationally more intensive.

The promise of LSS to diagnose dysplasia and CIS were tested in *in vivo* human studies in four different organs and in three different types of epithelium: columnar epithelia of the colon and Barrett's esophagus, transitional epithelium of the urinary bladder, and stratified squamous epithelium of the oral cavity.¹¹ All clinical studies were performed during routine endoscopic screening or surveillance procedures. In all of the studies, an optical fiber probe delivered white light from a xenon arc lamp to the tissue surface and collected the returned light. The probe tip was brought into gentle contact with the tissue to be studied. Immediately after the measurement, a biopsy was taken from the same tissue site. The biopsied tissue was prepared and examined histologically by an experienced pathologist in the conventional manner. The spectrum of the reflected light was analyzed and the nuclear size distribution determined. The majority of the distributions of dysplastic cell nuclei extended to a larger size.

These size distributions were then used to obtain the percentage of nuclei larger than 10 microns, and the total number of nuclei per unit area (population density). As noted above, these parameters quantitatively characterize the degree of nuclear enlargement and crowding, respectively. Figure 2.18 displays these LSS parameters in binary plots to show the degree of correlation with histological diagnoses. In all four organs, there is a clear distinction between dysplastic and nondysplastic epithelium. Both dysplasia and CIS have a higher percentage of enlarged nuclei and, on average, a higher population density, which can be used as the basis for spectroscopic tissue diagnosis.

In these clinical studies, LSS has been restricted to sampling of millimeter-size regions of tissue using a contact probe. To render this technology more practical for clinical applications, one needs to extend its capabilities to analyze wide areas of epithelial linings of the body. Recently, several novel technologies have been developed that bridge spectroscopy and imaging, i.e., spectroscopic imaging. In these imaging modalities each pixel or voxel of the imaged object, surface, or volume is represented not by a single number, as in conventional imaging, but by a linear array that is a spectrum of light scattered elastically or inelastically or transmitted through each pixel or voxel.

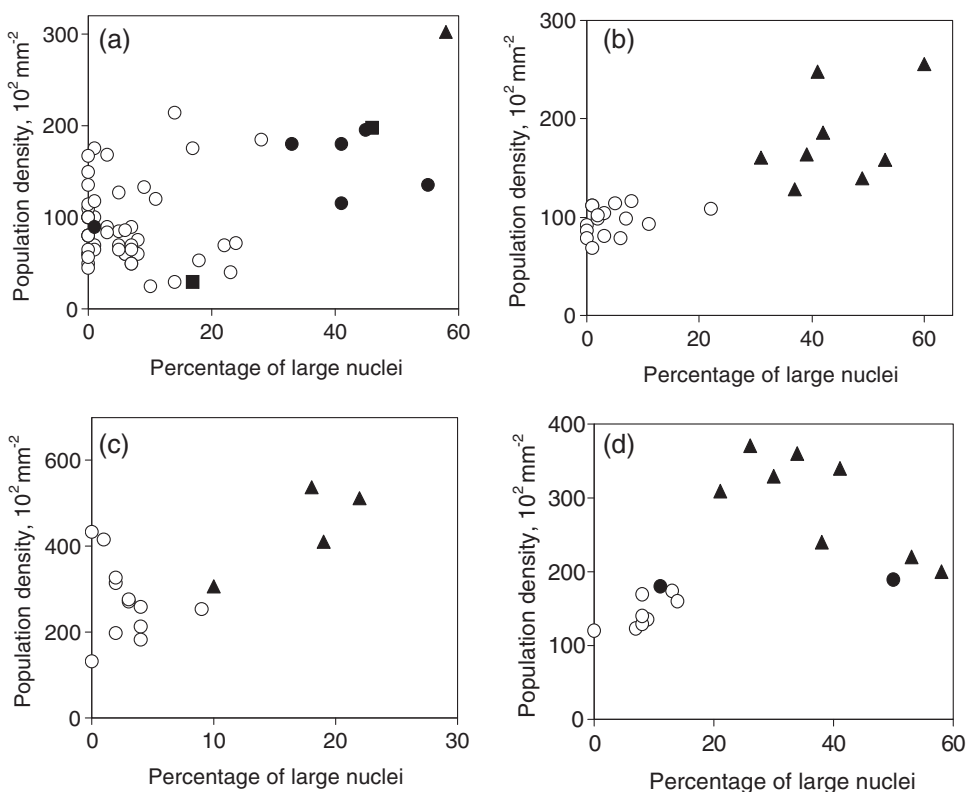


Figure 2.18 Dysplasia/CIS classifications for four types of tissue obtained clinically with LSS, compared with histologic diagnosis. In each case the ordinate indicates the percentage of enlarged nuclei and the abscissa indicates the population density of the nuclei, which parametrizes nuclear crowding. (a) Barrett's esophagus: nondysplastic Barrett's mucosa (○), indefinite for dysplasia (■), low-grade dysplasia (●), high-grade dysplasia (▲); (b) colon: normal colonic mucosa (○), adenomatous polyp (▲); (c) urinary bladder: benign bladder mucosa (○), transitional cell carcinoma *in situ* (▲); (d) oral cavity: normal (○), low-grade dysplasia (●), squamous cell carcinoma *in situ* (▲).

Kidder et al. and Cabib et al. developed Fourier transform infrared (FTIR) spectroscopic imaging to study the biochemical composition of tissues.^{53,54} Kidder et al. applied FTIR spectroscopic imaging to observe biochemical modifications in brain tissue.⁵⁵ Sowa et al. showed that spectroscopic imaging can be used to study tissue perfusion.⁵⁶ Farkas et al. developed a new modality of spectroscopic imaging by combining it with analytical cytology^{57,58} and applied spectral imaging for cancer detection and diagnosis.⁵⁹ In spectroscopic optical coherence tomography (OCT), the capabilities of OCT were enhanced by combining conventional OCT with Fourier transform spectroscopy.⁶⁰

LSS was extended to allow imaging applications as well.⁶¹ This LSS-based imaging allows mapping variations in the size of epithelial cell nuclei of living

tissues over wide surface areas. The resulting images provide direct quantitative measurements of nuclear enlargement and chromatin content, which can be translated into clinical diagnoses. The technique can be used for noninvasive or minimally invasive detection of precancerous changes in a variety of organs, such as the colon and oral cavity.

In LSS imaging, a light source with a broad illumination spectrum is used to illuminate the imaged tissue. The light from this source is collimated, polarized, and transmitted through one of several narrow-band filters to select the desired wavelengths covering the visible spectral range. A pair of equifocal achromatic lenses separated by twice their focal length collects the light backscattered by the sample. This so-called 4-f system ensures that the spatial distribution of light in the plane distanced one focal length between the collecting lenses depends on the angular distribution of light emerging from the tissue. Therefore, an aperture positioned at the center of the lens system determines the angular distribution of light scattered by the sample and collected by the CCD, which is placed one focal length away from the outer lens. The single scattering component is distinguished from the multiple scattering component by means of polarization discrimination using an analyzing polarizer, as in the polarization LSS. The CCD collects images for each of the illumination wavelengths. After all the filters are used, each pixel is represented by an LSS spectrum, which is analyzed using the Mie theory as in the other LSS modalities.

LSS imaging was applied to study *ex vivo* colon tissue samples that were obtained immediately after resection from patients undergoing colectomy for familial adenomatous polyposis. Colonic adenomas are precancerous dysplastic lesions exhibiting all of the characteristics of dysplastic lesions, including cell nuclear enlargement, pleomorphism, and hyperchromasia. The adenomas are surrounded by normal tissue covered by a single layer of epithelial cells. For each pixel ($25\ \mu\text{m} \times 25\ \mu\text{m}$) of the imaged field ($1.3\ \text{cm} \times 1.3\ \text{cm}$), the analysis of the LSS spectra enabled the size and refractive index of the nuclei in each pixel to be obtained. Then the imaged field was divided into $125\ \mu\text{m} \times 125\ \mu\text{m}$ regions and the percentage of nuclei larger than $10\ \mu\text{m}$ was obtained for each of these regions. As discussed above, this statistic, which characterizes the degree of nuclear enlargement, is highly significant for the diagnosis of dysplastic lesions in the colon and several other organs. The resulting color-coded plot is shown in Fig. 2.19. As expected, the nuclei are enlarged in the central, adenomatous region, but not in the surrounding nondysplastic tissue.

These results demonstrate that LSS has the potential to provide a means for detecting epithelial precancerous lesions and preinvasive cancers throughout the body. LSS is advantageous compared to conventional diagnostic techniques in that it can provide objective, quantitative results in real time without the need for tissue removal. The first clinical application

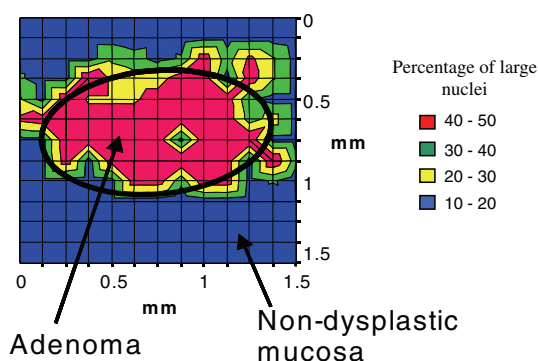


Figure 2.19 LSS images of colon tissue sample showing the spatial distribution of the percentage of enlarged nuclei. The adenoma observed histologically is marked by an ellipse. (See color plates.)

may be to guide random biopsies of previously undetectable, endoscopically invisible lesions. This could lead to new diagnostic and imaging technologies that would significantly improve the efficacy of cancer screening and surveillance procedures.

2.6.3 Imaging of early cancer and precancerous lesions with an endoscopic polarized scanning spectroscopy instrument

LSS-based detection of dysplasia in Barrett's esophagus (BE) has been demonstrated successfully using a simple proof-of-principle single-point instrument.^{10,11} This instrument was capable of collecting data at randomly selected sites, which were then biopsied. The data was processed off-line, and a comparison with biopsy results was made at a later time. The high correlation between spectroscopic results and pathology was sufficiently promising to justify the development of the clinical device, which is described herein.

A recently developed⁶² clinical endoscopic polarized scanning spectroscopy (EPSS) instrument is compatible with existing endoscopes (Fig. 2.20). It scans large areas of the esophagus chosen by the physician, and has the software and algorithms necessary to obtain quantitative, objective data about tissue structure and composition, which can be translated into diagnostic information in real time. This enables the physician to take confirming biopsies at suspicious sites and minimize the number of biopsies taken at non-dysplastic sites.

The instrument detects polarized light coming primarily from the epithelial layer. Although principally using the polarization technique to extract diagnostic information about dysplasia, the EPSS instrument also sums the two polarizations to permit the use of diffuse reflectance spectroscopy, which can also provide information about the early stages of adenocarcinoma.⁶³